Applied Surface Science 264 (2013) 45–51

Contents lists available at SciVerse ScienceDirect

Applied Surface Science

journal homepage: www.elsevier.com/locate/apsusc

Tribological behavior of electron beam D6ac weldment

Shyh-Chi Wu[a,b], Kuang-Hung Tseng[c,*], Hua-Chiang Wen[b], Ming-Jhang Wu[b], Chang-Pin Chou[b]

[a] Chung Shan Institute of Science and Technology, Taoyuan 325, Taiwan
[b] Department of Mechanical Engineering, National Chiao Tung University, Hsinchu 30010, Taiwan
[c] Institute of Materials Engineering, National Pingtung University of Science and Technology, Pingtung 91201, Taiwan

ARTICLE INFO

Article history:
Received 10 April 2012
Received in revised form 29 July 2012
Accepted 20 September 2012
Available online 26 September 2012

Keywords:
D6ac steel
Flow forming
Electron beam welding
Tempering
Tribological behavior

ABSTRACT

A flow formed D6ac steel tubing was joined using electron beam (EB) welding. Thereafter, the EB weldments were treated by tempering at temperatures of 450 °C and 550 °C. After tempering, the microstructural features, mechanical properties, and tribological characteristics of the EB D6ac weldment were studied. This study used a scratch test to evaluate the sliding wear resistance of the tempered weldment. Results indicate that the tempering softens the microstructure by reducing the dislocation density of the flow formed D6ac steel. For the 450 °C/2 h/air cooling tempering treated D6ac steel, the fracture toughness of the EB weldment can be significantly improved. The tribological behavior of the tempered D6ac weldment depended on the tempered microstructures.

1. Introduction

According to the SAE AMS 6431M standard, D6ac is a medium-carbon, low-alloy steel with a high hardenability that is primarily used in ultrahigh-strength structural applications. This type of steel provides a high yield strength/ultimate tensile strength (YS/UTS) ratio. However, the use of these steels is limited by their poor ductility at the highest mechanical strength levels [1]. These steels are produced using a consumable electrode vacuum arc melting process that offers optimum cleanliness and preferable ingot structures, providing optimum transverse mechanical properties.

This study uses two manufacturing processes: flow forming and EB welding. A flow forming process, also known as tube spinning or shear forming, is an advanced chipless metal forming process that is used to manufacture dimensionally precise, round, and seamless hollow components. In this process, the wall thickness is reduced as material is encouraged to flow mainly in the axial direction, increasing the length of workpiece. Flow forming is a cold working rotary-point extrusion technique for forming products with enhanced mechanical properties [2,3]. The flow forming process can form pre-hardened workpieces, thereby eliminating the difficulties and high costs associated with machining, grinding, and honing a hardened and distorted hollow component. The flow forming technique saves raw material, achieves rapid processing, and is cost competitive [4,5]. The flow forming process can be classified into two types of operations: forward and backward flow forming (Fig. 1).

The EB welding is a fusion welding process that produces a weld by impinging a beam of high-velocity, high-kinetic energy electrons to heat and melt the workpiece. Electrons are elementary atomic particles that are negatively charged and have extremely small masses. Raising electrons to a high energy state by accelerating them to approximately 30–70% of the speed of light creates sufficient energy to melt workpieces. The EB welding process is often performed in vacuum conditions to prevent the dissipation of the electron beam. In a vacuum, it is easy to accelerate free electrons and to control their orbits using electric and magnetic fields. Compared to other fusion welding processes, the EB welding offers the advantage of low heat input to the workpiece, resulting in the low distortion and low residual stress of the weldment [6]. The EB welding is becoming more common in the nuclear, chemical, and aerospace industries because of its high depth-to-width ratio and narrow heat-affected zone [7,8].

A post-weld heat treatment (PWHT) process is required to improve the mechanical properties of the weldment. The PWHT process can include many types of treatments. However, the two most common procedures used in steel fabrication are post heating and stress relieving. The PWHT process can improve the

* Corresponding author at: No. 1, Hseuhfu Rd., Neipu, Pingtung 91201, Taiwan. Tel.: +886 8 7703202; fax: +886 8 7740552.
E-mail address: tkh@mail.npust.edu.tw (K.-H. Tseng).

0169-4332/$ – see front matter © 2012 Elsevier B.V. All rights reserved.
http://dx.doi.org/10.1016/j.apsusc.2012.09.099

Table 1
Chemical composition (in wt.%, balance Fe) of D6ac steel.

Element	C	Mn	P	S	Si	Cr	Mo	Ni	V
Specification AMS 6431M	0.42–0.48	0.60–0.90	0.01	0.01	0.15–0.30	0.90–1.20	0.90–1.10	0.40–0.70	0.08–0.15
Used in the present work	0.47–0.48	0.76–0.84	0.01	0.01	0.27	0.98–0.99	1.02–1.10	0.55	0.10

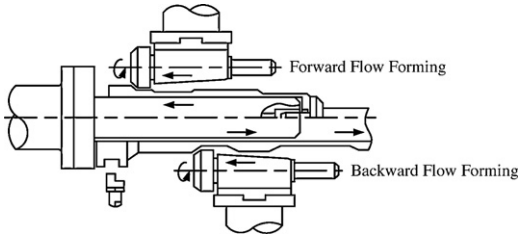

Fig. 1. Principle of flow forming processes.

performance of the weldments by adjusting the microstructure of weld metal. Extant literature offers limited data on the PWHT process for EB D6ac weldments. This information is critical to improving fracture toughness of the tempered weldment. Moreover, Wei et al. [9] examined the effect of tempering conditions on wear resistance of H13 steel. They concluded that the tempering conditions presented different influences on the wear resistance of steel in various wear mechanisms.

The scratch test is a new test method for evaluating the fracture toughness of materials. The scratch test consists of driving a probe, at a certain depth, through a material and is most likely the oldest mechanics-of-materials test for the mechanical characterization of materials. To study the fracture toughness of the tempered weldment, this study assessed the tribological behavior by determining the sliding wear resistance [10]. A flow formed D6ac steel tubing was welded using EB welding and subsequently tempering treated. This study used a scratch test to evaluate the sliding wear resistance of the tempered EB weldment. In addition, the scratch coefficient was used to characterize the wear resistance of the weldment.

2. Experimental details

The experiments in this study used D6ac steel, as specified by the standard AMS 6512C (double vacuum melted VIM-VAR). Table 1 shows the chemical composition of the experimental steel. The chemical composition of the D6ac steel was determined using energy dispersive X-ray spectrometer (EDS) and carbon and sulfur determination.

Prior to flow forming, the D6ac steel tubing was normalized by 910 °C/105 min/air cooling process parameters and machined to a wall of 6.0 mm thickness. Thereafter, it was further reduced to a wall of 2.1 mm thickness using forward flow forming. For the precision flow forming operations, the forward flow forming of the D6ac steel tubing was performed in a three-roller spinning machine (the three rollers were positioned in a 120° design with a spindle speed of 60 rpm and a feed rate of 0.7 mm rev^{-1}). Following flow forming, the tube received a solution treatment of 900 °C/30 min/air cooling.

Thereafter, a flow formed D6ac steel tube was EB welded in a vacuum chamber at a pressure of 1.33×10^{-2} Pa. Table 2 shows the EBW process parameters. The welding process used a heat input of 66.5 J mm^{-1}. To investigate their mechanical properties, the EB D6ac weldments were tempered at temperatures of 450 °C and 550 °C for 2 h, followed by air cooling.

Table 2
Process parameters of EB welding.

Accelerating voltage, kV	120
Beam current, mA	200
Vacuum level, Pa	1.33×10^{-2}
Focal length, mm	444.5
Speed, mm min^{-1}	2100
Pass number	1

A tensile test was used to determine the mechanical properties of the tempered EB weldments. Standard tensile specimens were constructed from the longitudinal direction of the tube and were milled to final dimensions that followed ASTM E370 specifications (Fig. 2). The gauge length of each specimen was 50.8 mm. The tensile test involved two strain rates: 0.2 (mm mm^{-1}) min^{-1}, which was used prior to the yield point, and 2 (mm mm^{-1}) min^{-1}, which was used after the yield point. In this experiment, three specimens were used for each test condition. The fracture surfaces of the tensile specimens were studied using a scanning electron microscopy (SEM).

The microstructural characterizations of the tempered EB weldments were examined using optical microscopy (OM), SEM, and transmission electron microscopy (TEM). All of the metallographic samples were prepared using standard procedures, including mounting, grinding, and polishing them to a 0.05 μm finish, followed by etching with natal (3% HNO_3 solution in alcohol). The tribological properties of the weldments were determined by the scratch test performed using an atomic force microscopy (AFM) in conjunction with the nanoindentation measurement system, which was operated at a constant scan speed of 2 μm s^{-1}. To determine scratch coefficients of the samples that were initiated in low ramp-force mode sliding cycles, the samples were subjected to ramped loads of 500 μN. Using this approach, the corresponding surface profiles were obtained, and 10 μm long scratches were formed using the constant force mode. The rough tip with a radius of 2 mm was applied to the samples at room temperature to avoid an impact cracking event. An X-ray diffractometer (XRD) with a Cu-Kα radiation source (λ = 0.15418 nm) was utilized to identify the crystalline of the phases present in weld metal.

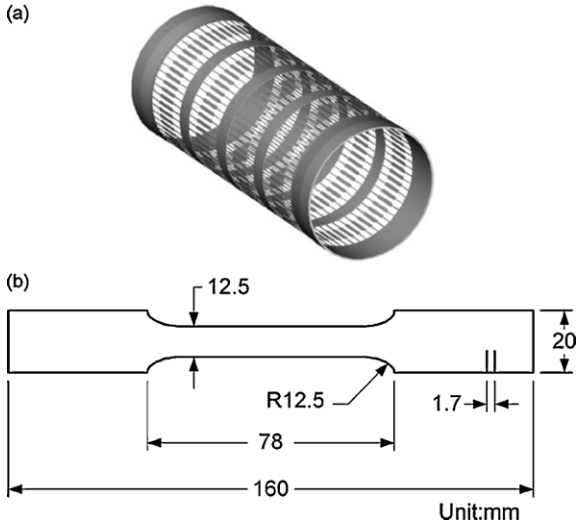

Fig. 2. Tensile specimen of EB welded tube. (a) Layout for procurement of tensile specimens and (b) dimensions of tensile specimen prepared in compliance with ASTM E370.

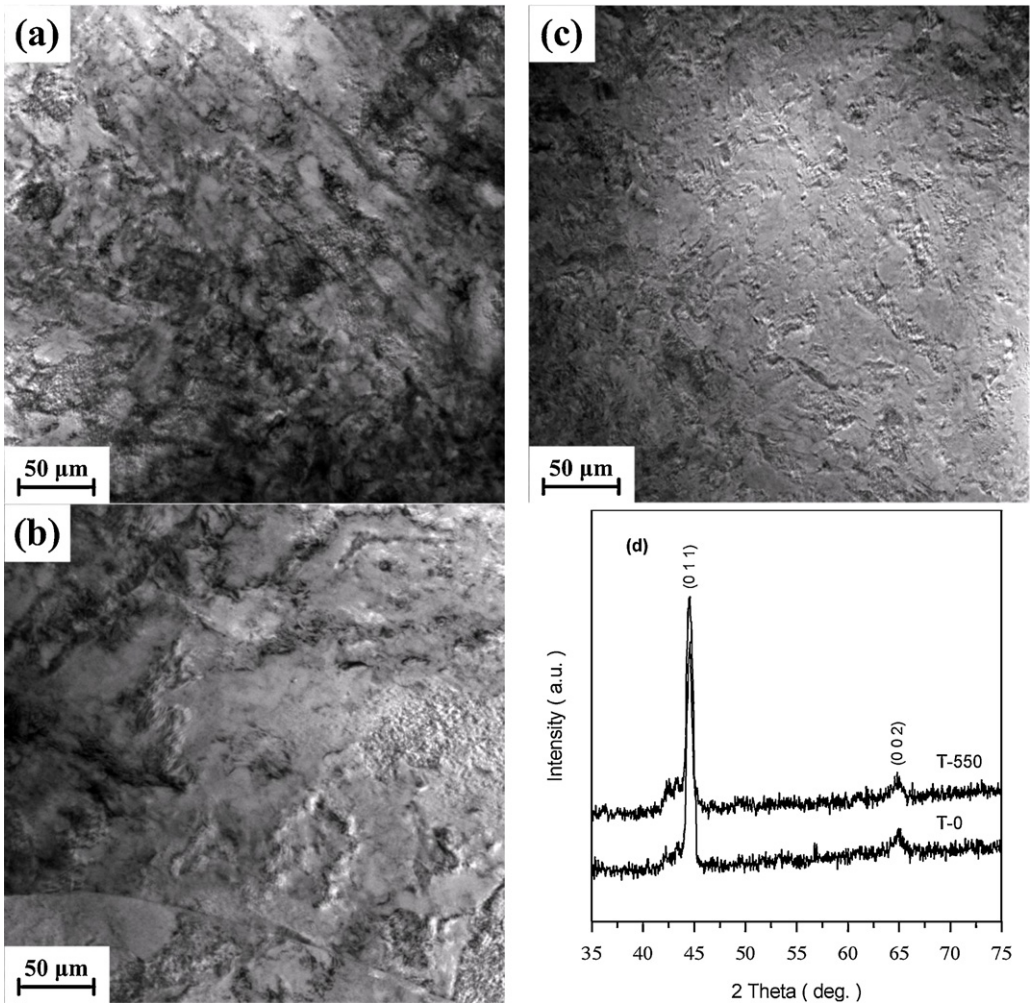

Fig. 3. TEM images of EB D6ac weldments subjected to various tempering conditions. (a) Without tempering, and tempered at various temperatures: (b) 450 °C and (c) 550 °C; (d) XRD pattern of tempered weldment at T-0 and T-550 conditions.

3. Results and discussion

3.1. Microstructural features of tempered weldment

Fig. 3a shows a plane-view TEM image of the EB D6ac weldment without tempering, displaying the numerous misfit dislocations from the work hardening. The result shows that the flow formed D6ac weldment exhibits a high dislocation density. When D6ac steel is subjected to flow forming, the dislocation density increases due to the formation of new dislocations and dislocation multiplication [11]. The dislocation densities gradually decreased when the EB D6ac weldment was tempered at 450 °C (Fig. 3b). A few dislocations were observed when the weldment was being tempered at 550 °C (Fig. 3c). The gradual change in the microstructure of the EB weldments indicated that the tempering process softens the microstructure by reducing the dislocation density of the flow formed D6ac weldment. Fig. 3d shows the XRD patterns of the EB D6ac weldments obtained without tempering and tempered at 550 °C. The relative peak intensities of the T-0 and T-550 conditions corresponded to the positions at 44.58° (0 1 1) and 64.98° (0 0 2), respectively. The maximum intensity under the T-0 condition was observed in the (0 1 1) peak position. The peak intensities of α' phase under the T-550 condition were the same as those in the T-0 condition. In this work, the wall thickness of D6ac steel tubing was reduced to 65% using forward flow forming technique. The result shows that the large cold working deformations of D6ac steel can result in formation of deformation-induced martensite.

3.2. Mechanical properties of tempered weldment

The result of the microstructural features is strongly correlated to the mechanical properties of the weldment. Table 3 shows the tensile test results of the EB D6ac weldments subjected to various tempering temperatures. The weldment without tempering exhibited lower mechanical strength (the average values of the YS and UTS are approximately 380 MPa and 608 MPa, respectively)

Table 3
Mechanical properties of EB D6ac weldments subjected to various tempering conditions.

Sample code	Heat treatment conditions	YS (0.2% offset) (MPa)	UTS (MPa)	Elongation (%)
T-0	EB weldment without tempering	380	608	0.5
T-450	EB weldment tempering 450 °C	1319	1443	9.1
T-550	EB weldment tempering 550 °C	1239	1309	10.6

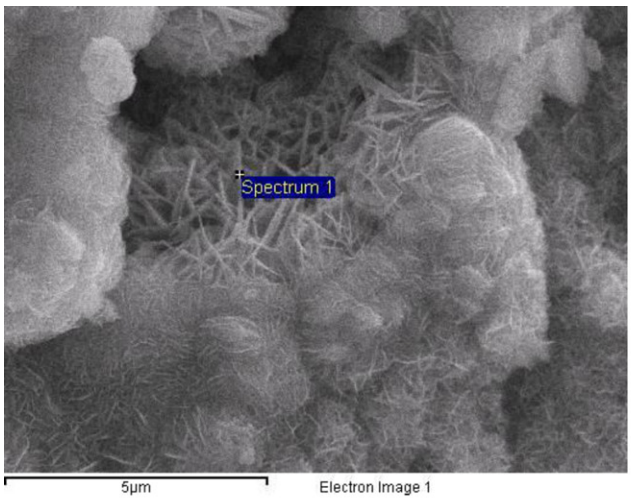

(a) T-0 condition

Element	wt.%	at.%
C K	17.76	39.40
O K	18.06	30.09
Fe K	64.18	30.51
Totals	100	100

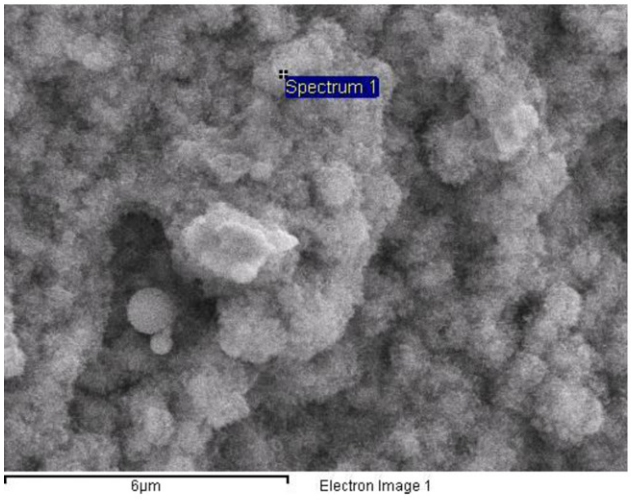

(b) T-450 condition

Element	wt.%	at.%
C K	9.26	29.63
O K	4.62	11.10
Fe K	86.12	59.27
Totals	100	100

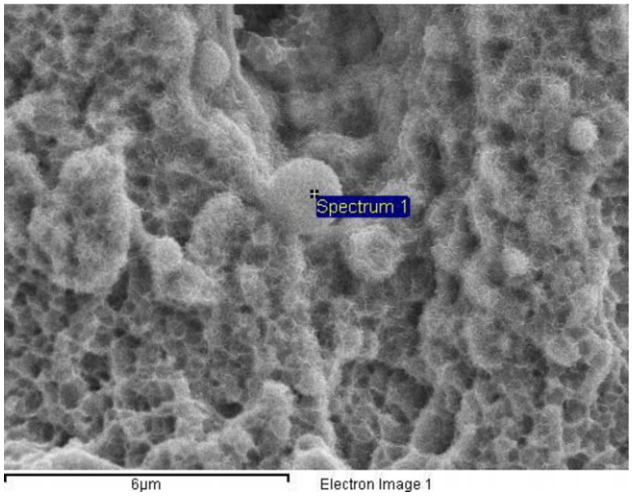

(c) T-550 condition

Element	wt.%	at.%
C K	2.45	9.92
O K	2.35	7.15
Fe K	95.20	82.93
Totals	100	100

Fig. 4. SEM photos of tensile specimen of EB D6ac weldments subjected to various tempering conditions. (a) Without tempering, and tempered at various temperatures: (b) 450 °C and (c) 550 °C.

and elongation (an average value of 0.5%). The result indicates mechanical properties that do not meet specification requirements. As a result, the EB D6ac weldment requires further tempering treatment to improve its mechanical properties and meet specifications. The YS of the weldment tempered at temperatures of 450 °C exceeded the 1310 MPa value stipulated by SAE AMS 6431 M. However, the YS of the weldment tempered at temperatures of 550 °C decreased significantly. Subsequently, the UTS of the weldment tempered at temperatures of 450 °C and 550 °C are lower than the SAE AMS 6431M specification of 1517–1724 MPa. The elongation of the tempered weldments specifically increases in the range of 9.1–10.6% (under T-450 and T-550 conditions). The

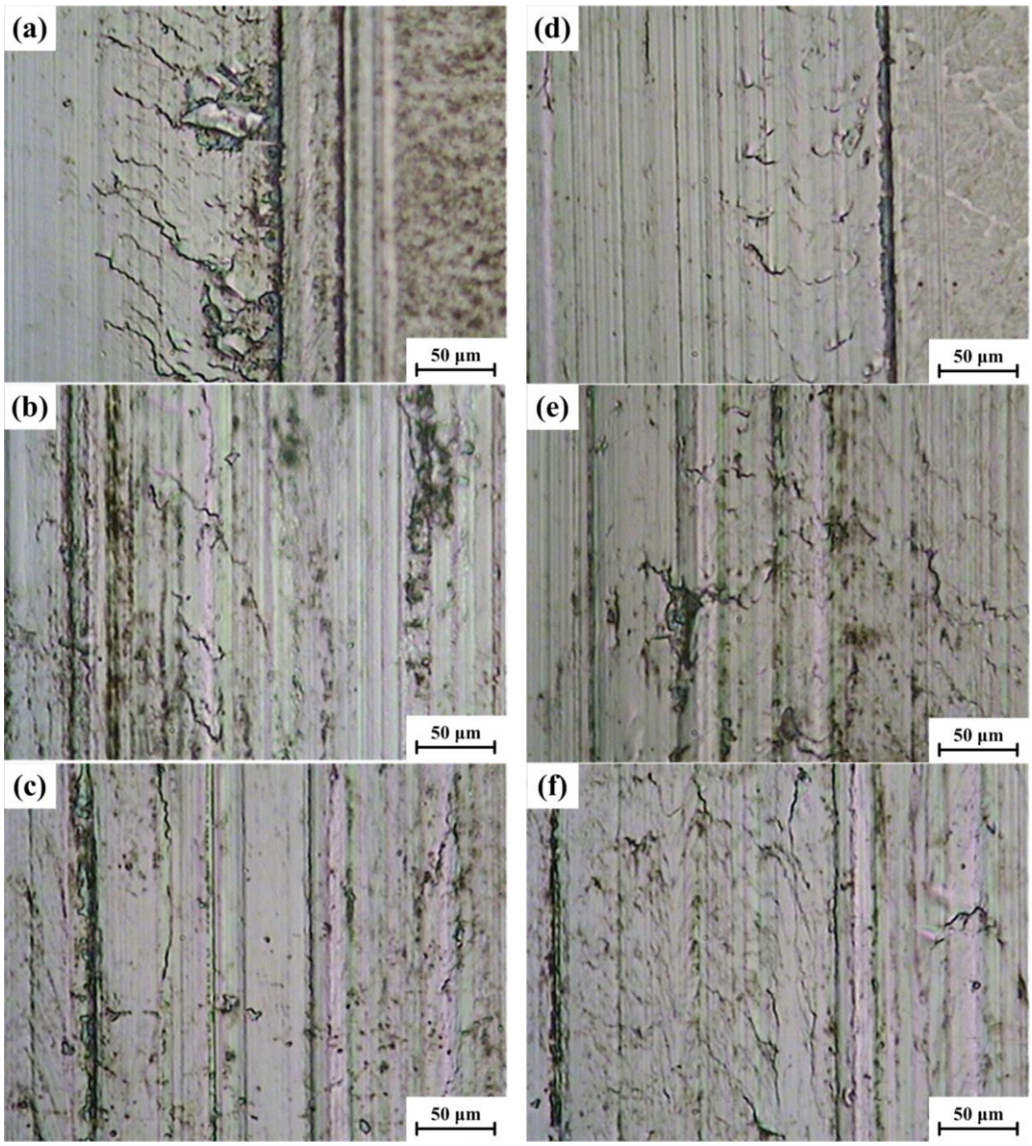

Fig. 5. OM photos of sliding wear of EB D6ac weldments subjected to various tempering conditions. Base metals at (a) T-0, (b) T-450, (c) T-550 conditions; weld metals at (d) T-0, (e) T-450, (f) T-550 conditions.

fracture toughness of the tempered D6ac weldment is significantly higher than that of the weldment without tempering. Chang et al. [12] concluded that the fracture characteristics of D6ac steels with relatively coarse and discrete carbides at the prior-austenite grain boundaries were observed after tempering at high temperatures. Also, Narasimha Rao et al. [13] and Abbaszadeh et al. [14] reported that fracture toughness of alloy steels can be improved significantly when a bainite, tempered martensite, or mixed bainite/martensite microstructure forms instead of a fully martensite microstructure.

Fig. 4 shows the SEM fractographs of the tensile specimens tempered at various temperatures. An EDS analysis shows the weight and atomic percent compositions. The C element (at.%) decreased from 39.40% to 9.92%, and the Fe element (at.%) increased from 30.51% to 82.93% when tempering conditions changed from the T-0 condition to the T-550 condition. Based on the high content of C element (Fig. 4a), the needle-like morphology can be attributed as a martensite. Tempering alters the size and distribution of carbides in the martensite, forming a tempered martensite. The result shows that the martensite can be changed into the tempered martensite after tempering at 450 °C and 550 °C, and the low content of C element was displayed (Fig. 4b and c). The time–temperature–transformation (TTT) diagram of D6ac steel shows that the martensite start (Ms) temperature is approximately 300 °C [15]. Consequently, the D6ac steel was tempered at a relatively high temperature (exceeds Ms temperature) where retained austenite will be converted to either fresh martensite or bainite.

3.3. Tribological characteristics of tempered weldment

Wei et al. [9] concluded that the wear resistance strongly depended on the tempered conditions of the steels. To investigate the tribological behaviors of the EB D6ac weldments subjected to various tempering conditions, the friction plots obtained from the base metal and the weld metal were compared. The primary results of the sliding wear characteristics and the in situ lateral force were revealed. All of the abraded specimens were initiated at a constant force during the sliding cycles. Fig. 5 shows the OM photos of the sliding wear of the EB D6ac weldment subjected to various tempering temperatures. The observable damage resulted from the asperity tip on the metal surface, with shearing and rupturing of the adhesive surface as a result of local contact pressure during sliding. Fig. 5a reveals that the wear debris generated in the

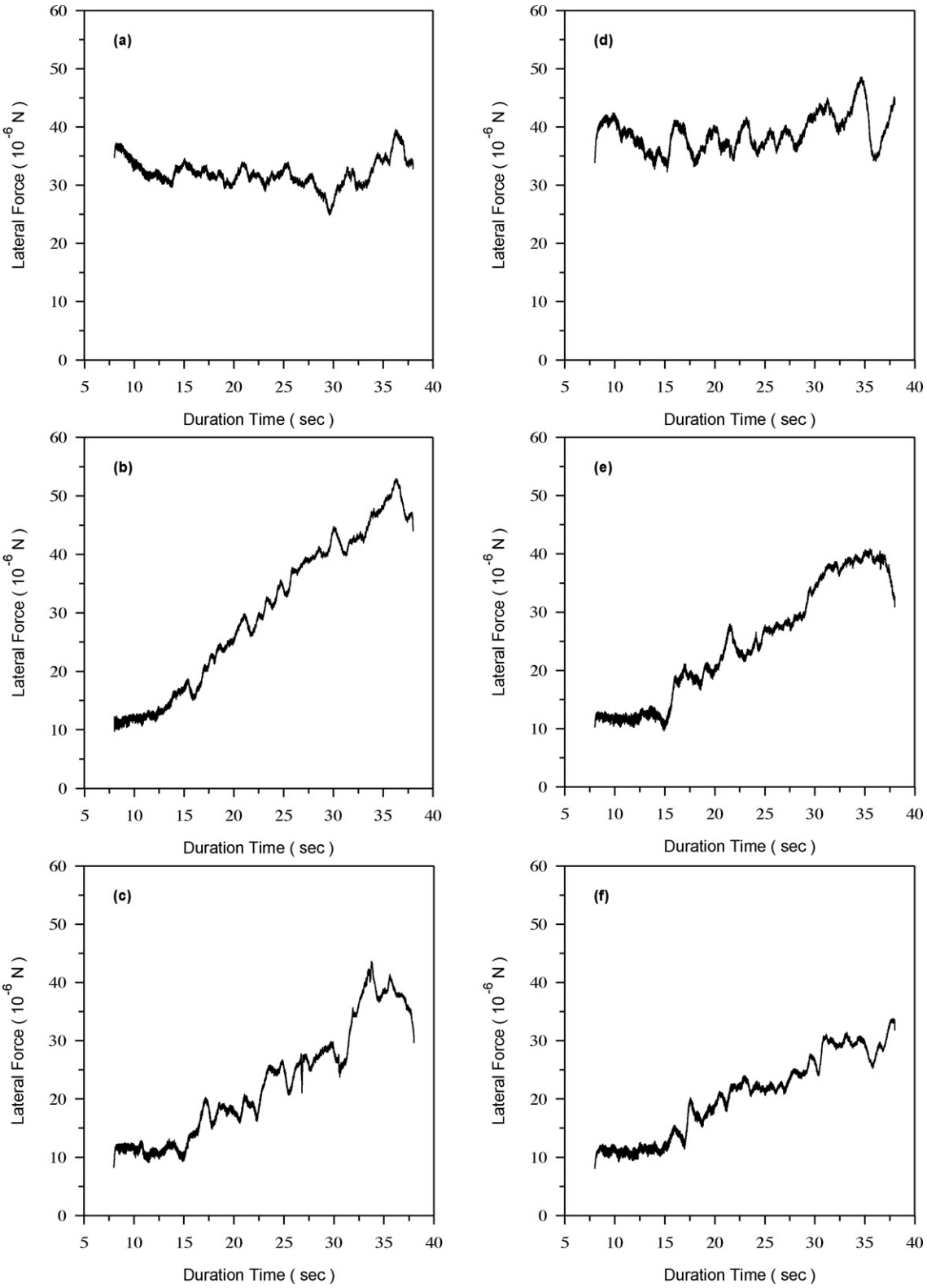

Fig. 6. Plots of fluctuations in lateral force with respect to duration time of EB D6ac weldments subjected to various tempering conditions. Base metals at (a) T-0, (b) T-450, (c) T-550 °C conditions; weld metals at (d) T-0, (e) T-450, (f) T-550 conditions.

sliding process. The scratches are the typical characteristic of adhesive wear. Fracture damage rapidly increases with curved cracks aligned approximately perpendicular to the direction of scratching when being tempered from the T-450 condition to the T-550 condition (Fig. 5b and c). In a single pass weld, some crack fractures occurred in the weld metal. The scratch fractures appeared to be associated with the boundaries between the original phases (Fig. 5d). However, for weld metals that were tempered at both the T-450 and T-550 conditions, ductility damage occurred on the worn surface. There was a relatively smooth surface and a

Table 4
Scratch coefficients of EB D6ac weldments subjected to various tempering conditions.

Sample code	Heat treatment conditions	Scratch coefficients	
		Base metal	Weld metal
T-0	EB weldment without tempering	0.336	0.119
T-450	EB weldment tempering 450 °C	0.273	0.139
T-550	EB weldment tempering 550 °C	0.132	0.110

regular outline of the scratch area (Fig. 5e and f). There was evidence of carbide grain break-up and the fracturing of the scratch surface in the T-0 condition (Fig. 5a). The scratched surfaces suffered gross failures in the base metal and soft cracks in the weld metal after tempering.

Fig. 6 shows the fluctuations in the lateral force with respect to duration time. Fig. 6a shows the stable lateral force on the base metal for the loads below 40 μN. The lateral force gradually increased to 50 μN because of the increase in the fracture toughness in the base metals tempered from the T-450 condition to the T-550 condition (Fig. 6b and c). Eventually, the scratched surface suffered from brittleness to ductility damage in the base metal. Fig. 6d shows the stable lateral force on the weld metal for the loads over 40 μN. However, irregular fluctuations were observed compared to the samples under the T-450 and T-550 conditions (Fig. 6e and f). The lateral forces in the T-450 and T-550 samples were gradually tested up to 50 μN. This study suggests that tempering treatments increase the elongation of the weld metal because the treatments cause the deformation-induced martensite to transform into the tempered martensite (which is composed of spheroidized carbide dispersed in ferrite matrix) during high-temperature tempering. This study attributes this behavior to the ferrite contained in weld metal.

The results of the EB D6ac weldments at T-0, T-450, and T-550, respectively, were 0.336, 0.273, and 0.132 for the scratch coefficients of the base metal, and 0.119, 0.139, and 0.110, respectively, for the weld metal. These results are shown in Table 4 and support the trend of the tempering effect and provide a reasonable estimate of the magnitude of the scratching damage to the base metal and weld metal. The tribological behavior of the tempered D6ac weldment depended on the tempered microstructures. This study has systematically illustrated that microstructural features influence their lateral force and scratch coefficients of the EB D6ac weldments subjected to various tempering conditions. The tribological characteristics from the base metal and weld metal were determined.

4. Conclusion

Seamless tubing of D6ac steel manufactured using flow forming technique was joined using EB welding process. Various tempering conditions were conducted to investigate the microstructural features, mechanical properties, and tribological characteristics of the EB D6ac weldments. The following points summarize the experimental results:

1. Cold working causes deformation-induced martensite. Tempering treatment softens the microstructure of the flow formed D6ac steel by reducing the dislocation density.

2. The fracture toughness of the tempered D6ac weldment is significantly higher than that of the weldment without tempering. For the 450 °C/2 h/air cooling tempering treated D6ac steel, the fracture toughness of the EB weldment can be significantly improved.

3. The scratch tests were found to vary somewhat in sensitivity with respect to the base metal and the weld metal. The tribological behavior of the tempered D6ac weldment depended on tempered microstructures. There was an increase in scratch coefficients from the tempering because the deformation-induced martensite transformed into the tempered martensite.

Acknowledgments

The authors gratefully acknowledge the financial support provided to this study by the National Science Council under the grant no. 99-2221-E-009-031-MY2 and the National Nano Device Laboratories under the grant no. 99-C03S-042, Taiwan. In this experimental work, SEM and TEM were performed in the Precision Instruments Center of NPUST.

References

[1] A. Salemi, A. Abdollah-Zadeh, M. Mirzaei, H. Assadi, A study on fracture properties of multiphase microstructures of a CrMo steel, Mater. Sci. Eng. A 492 (2008) 45–48.
[2] M. Jahazi, G. Ebrahimi, The influence of flow-forming parameters and microstructure on the quality of a D6ac steel, J. Mater. Process. Technol. 103 (2000) 362–366.
[3] M.S. Mohebbi, A. Akbarzadeh, Experimental study and FEM analysis of redundant strains in flow forming of tubes, J. Mater. Process. Technol. 210 (2010) 389–395.
[4] Y.J. Lee, M.C. Kung, I.K. Lee, C.P. Chou, Effect of lath microstructure on the mechanical properties of flow-formed C-250 Maraging steels, Mater. Sci. Eng. A 454–455 (2007) 602–607.
[5] Y.J. Lee, S.C. Wu, J.L. Chang, C.P. Chou, I.K. Lee, Effects of stress relief coupled with reduced EBW energy on flow-formed Maraging steel weldment, Sci. Technol. Weld. Join. 13 (5) (2008) 462–466.
[6] P. Lacki, K. Adamus, Numerical simulation of the electron beam welding process, Comput. Struct. 89 (2011) 977–985.
[7] R. Rai, T.A. Palmer, J.W. Elmer, T. DebRoy, Heat transfer and fluid flow during electron beam welding of 304L stainless steel alloy, Weld. J. 88 (2009) 54s–61s.
[8] R. Lindau, M. Klimenkov, U. Jäntsch, A. Möslang, L. Commin, Mechanical and microstructural characterization of electron beam welded reduced activation oxide dispersion strengthened—Eurofer steel, J. Nucl. Mater. 416 (2011) 22–29.
[9] M.X. Wei, S.Q. Wang, L. Wang, X.H. Cui, K.M. Chen, Effect of tempering conditions on wear resistance in various wear mechanisms of H13 steel, Tribol. Int. 44 (2011) 898–905.
[10] C.R.F. Azevedo, E.R. Marques, Three-dimensional analysis of fracture, corrosion and wear surfaces, Eng. Fail. Anal. 17 (2010) 286–300.
[11] S.C. Wu, H.C. Wen, M.J. Wu, C.P. Chou, Fracture responses of microstructures of electron beam-welded D6AC, Vaccum 86 (2012) 1828–1833.
[12] T.L. Chang, L.W. Tsay, C. Chen, Influence of gaseous hydrogen on the notched tensile strength of D6AC steel, Mater. Sci. Eng. A 316 (2001) 153–160.
[13] T.V.L. Narasimha Rao, S.N. Dikshit, G. Malakondaiah, P. Rama Rao, On mixed upper bainite–martensite in an AISI 4330 steel exhibiting an uncommonly improved strength-toughness combination, Scripta Metall. Mater. 24 (1990) 1323–1328.
[14] K. Abbaszadeh, H. Saghafian, S. Kheirandish, Effect of bainite morphology on mechanical properties of the mixed bainite–martensite microstructure in D6ac steel, J. Mater. Sci. Technol. 28 (2012) 336–342.
[15] G.L. Peterman, How to heat treat D6ac steel, Met. Prog. 87 (1965) 80–83.